Inorganic Chemistry

Communication

pubs.acs.org/IC

Unexpected Competition between Antiferromagnetic and Ferromagnetic States in $Hf_2MnRu_5B_2$: Predicted and Realized

Pritam Shankhari,[†] Yuemei Zhang,[†] Dejan Stekovic,[†,‡] Mikhail E. Itkis,[†,‡,§] and Boniface P. T. Fokwa*[,†,§]

[†]Department of Chemistry, [‡]Center for Nanoscale Science and Engineering, and [§]Department of Chemical and Environmental Engineering, University of California, Riverside, California 92521, United States

Supporting Information

ABSTRACT: Materials "design" is increasingly gaining importance in the solid-state materials community in general and in the field of magnetic materials in particular. Density functional theory (DFT) predicted the competition between ferromagnetic (FM) and antiferromagnetic (AFM) ground states in a ruthenium-rich $Ti_3Co_5B_2$-type boride ($Hf_2MnRu_5B_2$) for the first time. Vienna ab initio simulation package (VASP) total energy calculations indicated that the FM model was marginally more stable than one of the AFM models (AFM1), indicating very weak interactions between magnetic 1D Mn chains that can be easily perturbated by external means (magnetic field or composition). The predicted phase was then synthesized by arc-melting and characterized as $Hf_2Mn_{1-x}Ru_{5+x}B_2$ (x = 0.27). Vibrating-scanning magnetometry shows an AFM ground state with $T_N \approx 20$ K under low magnetic field (0.005 T). At moderate-to-higher fields, AFM ordering vanishes while FM ordering emerges with a Curie temperature of 115 K. These experimental outcomes confirm the weak nature of the interchain interactions, as predicted by DFT calculations.

Recent research efforts in solid-state and materials chemistry are concerned with the design and prediction of new compounds and materials. However, it is difficult, in general, to design a phase a priori, and in most cases, the ability to broadly design and predict new phases with new structures remains a challenge.[1−4] On the one hand, "materials design" for a known structure type is possible, e.g., by isoelectronic elemental substitutions, intercalation of species into solids, or synthesis of coordination solids based on solid-state structures to achieve interesting physical properties.[5] As proposed by Canfield,[6] to design a material that will exhibit a specific property, there often needs to be some model or idea of which parameters are important and how to influence or control them. This guiding principle is often an admixture between theory and practical concerns, such as which elements or compounds can readily—and safely—be used: For an intermetallic material with magnetic properties, for example, the tendency is to look at compounds with 3d magnetically active transition metals and/or rare-earth (4f) elements.[6]

Transition-metal borides crystallizing in several unique structures have been the focus of extensive research interest in recent years because of their interesting itinerant magnetic properties.[7−12] $Ti_3Co_5B_2$[13] is one such prolific structure type that has produced many compounds, including ternaries ($A_3T_5B_2$), quaternaries ($A_2MT_5B_2$), and quinaries [$A_2M(TT')_5B_2$]. The ternary variants $A_3T_5B_2$ are formed by face-connected trigonal, tetragonal, and pentagonal prisms of T atoms (generally electron-rich and smaller transition metals such as Co, Rh, Ir, and Ru). The A atoms (relatively large atoms such as Mg, Sc, Ti, Zr, and Hf) reside inside both tetragonal and pentagonal prisms, while the B atoms are coordinated within the trigonal prisms.[14] In quaternaries (see Figure 1a) and quinaries, magnetically active

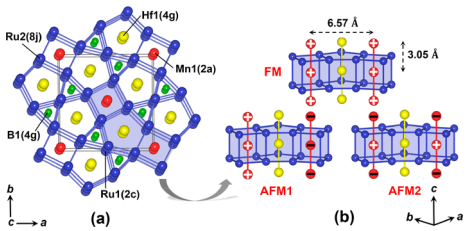

Figure 1. (a) Representative view of the structure of $Hf_2MnRu_5B_2$ along [001] and (b) different magnetic models for Mn chains. The + and − signs represent opposite types of spins.

M atoms sitting inside the tetragonal prisms build chains along [001] with intrachain M−M distances in the range 2.90−3.10 Å (see Figure 1b) suitable for magnetic interactions. Both experimental and theoretical studies[15−21] have been conducted extensively on the magnetic properties of such quaternaries and quinaries and have revealed that magnetic M atoms in conjunction with the electronic contributions from T atoms can drastically influence the magnetic properties. For example, in the quinary series $Sc_2FeRh_{5-x}Ru_xB_2$ and $Sc_2FeIr_{5-x}Ru_xB_2$, the evolution of magnetic interactions has been observed experimentally and reproduced theoretically as a function of the valence electron count (VEC): Preferred antiferromagnetic (AFM) coupling was found below VEC = 62, while preferred ferromagnetic (FM) coupling was found at VEC = 63 or higher.[17,18,21] In general, Fe-based magnetic materials have been studied, and it is understood that, in these phases, dominating FM interactions are found in systems with valence-electron-richer 4d/5d transition metals (T = Rh, Ir), while dominating AFM interactions are observed in those containing valence-

Received: July 13, 2017

DOI: 10.1021/acs.inorgchem.7b01758
Inorg. Chem. XXXX, XXX, XXX−XXX

electron-poorer 4d transition-metal (T = Ru)-based systems. The Mn-based compounds studied to date are all Rh- or Ir-rich, and their magnetic properties fit well within the studied VEC range. However, no Mn-based Ru-rich phase of this structure type is known. Mn has produced some important magnetic materials such as Mn_3GaC, hard ferromagnets MnBi,[22] Mn_2Ga_5[23] and MnB[24] even though its ground state is AFM. Herein, we report on the design of the first Mn-based Ru-rich phase, $Hf_2MnRu_5B_2$, predicted theoretically to show competing AFM and FM ordering states and successfully synthesized and investigated for its magnetic properties.

The recipe for designing this phase was clear: It should be Ru-rich and should incorporate Mn along with a 4d or 5d element. Because $Hf_3Ru_5B_2$ was already reported,[25] this phase was used as the starting point. At first, we employed density functional theory (DFT) calculations to investigate the electronic structure, bonding, and magnetic interactions in $Hf_2MnRu_5B_2$. Geometry optimization was performed on a nonmagnetic (NM) model of $Hf_2MnRu_5B_2$ using the projector-augmented wave method of Blöchl[26,27] coded in the Vienna ab initio simulation package (VASP).[28] Using the geometry-optimized structures, three different magnetic models were designed (Figure 1b), and spin-polarized VASP calculations were performed to investigate their spin-exchange interactions. The structural parameters were further allowed to relax while the spin-polarized VASP calculations were performed. Table S5 summarizes the results of the VASP calculations. All three spin-polarized models were energetically much more stable than the NM model, indicating favoring of spin interactions in the system. Among the three spin-polarized models, FM and AFM1 were found to be significantly more stable than the AFM2 model, indicating that FM interaction of the spins within the individual chains is preferred. Interestingly, the FM and AFM1 models were energetically very close in energy (the FM model was more stable just by 3.86 meV/u.c.), which seemed somewhat surprising to us because until now in all calculations in the Ru-rich phases of this structure type, which were done mainly on Fe-based phases, AFM1 was calculated to be the most stable model. For example, the recent DFT calculations on $Zr_2FeRu_5B_2$ indicated that AFM1 is more stable than FM by 120 meV/u.c., while in $Ti_2FeRu_4RhB_2$, AFM1 is found to be more stable than FM by 61.1 meV/u.c.[29,30] Furthermore, considering the 61 VEC for $Hf_2MnRu_5B_2$, it would favor dominating AFM interactions as mentioned earlier (VEC < 62). Certainly, either Mn or Hf or both act as a rule breaker in $Hf_2MnRu_5B_2$. Therefore, this unexpected prediction had to be verified experimentally (see below).

VASP results on the FM ground state show a large moment of 2.70 μ_B on Mn, which was mainly attributed to the splitting of the majority and minority spins of Mn d orbitals (Figure 2b). Also, very small moments were calculated on Ru atoms (Table S5).

$Hf_2MnRu_5B_2$ was synthesized by arc-melting the elements under an argon atmosphere. Structure refinement and phase analysis of the powder X-ray data were done by the Rietveld method,[31,32] which yielded a mixed occupancy of Ru and Mn at the 2a Wyckoff position and a final composition of $Hf_2Mn_{0.73(1)}Ru_{5.27(1)}B_2$. A Fe/Ru mixed occupancy was also observed in the isostructural $Zr_2FeRu_5B_2$ and related systems.[29] The results of the Rietveld refinement are given in Tables S1–S3 and Figure S1. The main phase $Hf_2Mn_{0.73}Ru_{5.27}B_2$ was produced with 92 wt % along with minor known side phases identified as HfRu (4.6 wt %) and $Ru_{1-x}Mn_x$ (x = 0.40 and 3.4 wt %). The refined lattice parameters a = 9.3021(5) Å and c = 3.0549(2) Å are in good agreement with those optimized by DFT (Table S1).

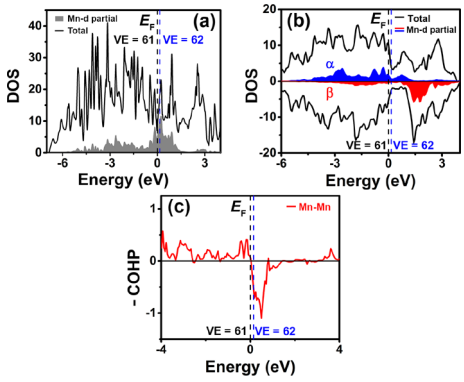

Figure 2. (a) Non-spin-polarized and (b) spin-polarized [majority (blue) and minority (red) spin states of Mn] density of state curves of $Hf_2MnRu_5B_2$ (VEC = 61). (c) Non-spin-polarized COHP curve for the Mn–Mn interaction. The Fermi level (E_F) is shown as a black dotted line (VEC = 61), while the blue dotted line represents the Fermi level for VEC = 62.

Experimental and structure determination details are provided in the Supporting Information.

Magnetization measurements were carried out in a vibrating-sample magnetometer in the field-cooled (FC) and zero-field-cooled (ZFC) modes and at different magnetic fields (Figure 3).

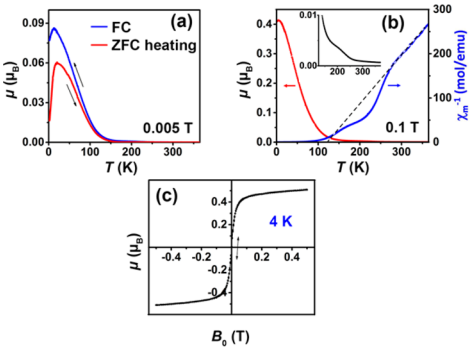

Figure 3. Magnetization versus temperature and inverse susceptibility versus temperature plots for $Hf_2Mn_{0.73}Ru_{5.27}B_2$ at (a) 0.005 and (b) 0.1 T fields. (c) Magnetization versus field strength curve (hysteresis loop) measured at 4 K up to an applied field of 0.5 T.

At very low field (0.005 T), a maximum (T_N = 20 K) is apparent for both FC and ZFC measurements in the μ–T plot (Figure 3a), indicating AFM ordering. However, this AFM transition vanishes at high magnetic fields (Figures 3b and S4), and a FM state emerges with $T_C \sim$ 115 K, indicating metamagnetic behavior for this compound. This behavior might be rationalized by the competition between the AFM1 and FM ground states and weak interchain Mn–Mn interactions, as found by DFT calculations. Our understanding is that the ground state is AFM with weak AFM interactions between the Mn chains. These weak interactions can be easily overcome by a small applied field. Indeed, at 0.1 T, a FM transition at $T_C \sim$ 115 K appears in the μ–T plot, indicating metamagnetic behavior for this compound. Also, a Curie–Weiss behavior, $\chi_m = C/(T - \theta)$, was apparent above 275 K for the $1/\chi_m$–T plot, the fitting of which led to a positive Weiss constant of 116.7 K, confirming the presence of FM interactions. The derived Curie constant (C) is 9.29×10^{-7} emu·K·mol^{-1}, which leads to an effective moment of 2.73 μ_B.

DOI: 10.1021/acs.inorgchem.7b01758
Inorg. Chem. XXXX, XXX, XXX–XXX

This moment is very close to the DFT-calculated moment on Mn for the two favored FM and AFM1 magnetic models (Table S5).

The $1/\chi_m - T$ plot at 0.1 T also indicates a deviation from the Curie–Weiss line between 150 and 275 K, also observed in the $\mu - T$ plot upon enlargement (inset in Figure 3b). This weak transition, which disappears at high magnetic fields (e.g., at 5 T; Figure S4b), is still unidentified but most probably arises from the metamagnetic nature of the phase. Furthermore, to confirm that the magnetic transitions of $Hf_2MnRu_5B_2$ are not originating from the side phase $Ru_{1-x}Mn_x$, we have successfully synthesized and measured the magnetic property of this phase, which was found to be Pauli paramagnetic with a magnetic moment 3 orders of magnitude weaker than that of $Hf_2MnRu_5B_2$ at 0.05 T.

To further understand the nature of Mn–Mn interactions within the chains, crystal orbital Hamilton population (COHP) analysis was performed. In the non-spin-polarized Mn–Mn COHP (Figure 2c) of $Hf_2MnRu_5B_2$, the Fermi level (E_F) falls in a nonbonding region; thus, direct Mn–Mn interactions would be predicted to be AFM within the chains.[33] However, a large antibonding peak is found near E_F in the non-spin-polarized Mn–Mn COHP plot (from 0.0 to 1.0 eV; Figure 2c). Assuming a valid rigid band approximation, E_F would shift to slightly higher energies with increased VEC for the experimental composition ($Hf_2Mn_{0.73}Ru_{5.27}B_2$ has 61.3 VEC compared to 61 for $Hf_2MnRu_5B_2$) and fall into the antibonding region. Consequently, COHP would predict direct FM Mn–Mn interactions (E_F for VEC = 62 is shown in Figure 2). This analysis also confirms the weak nature of the AFM interactions, which in this case would be suppressed by an increase of the VEC (a slight change in the composition).

Field-dependent measurements (see Figure 3c) at low temperature (4 K) revealed a hysteretic behavior with extremely small coercivity; thus, the compound can be classified as an extremely soft magnetic material. Even though the ground state is AFM below 20 K, the presence of hysteresis at 4 K indicates that a canting of the magnetic spins is very probable. Furthermore, the magnetic moment per Mn atom obtained from the $\mu - H$ plot is much smaller than the theoretically predicted value for a FM state, which also hints at a canted AFM ground state.

VASP spin–orbit coupling calculations indicated that spin parallel to the *c* axis is higher in energy than spin perpendicular to the *c* axis by 0.84 meV/u.c. (the energy difference for hard magnetic MnBi is 0.30 meV/u.c.), indicating large magnetic anisotropy. However, the interchain Mn–Mn spin-exchange interaction is very weak, making it very easy to flip the spins of each isolated FM Mn chain under an applied magnetic field, like the behavior of soft magnetic $Ti_2FeRh_3B_2$.[30] Therefore, this compound ends up having a very small coercivity despite its large magnetic anisotropy.

The VEC of this new compound is 61 (61.3 for the experimental composition), and thus it is surprising that FM interactions dominate in this compound, even if it is only at high magnetic fields. In fact, this behavior mostly occurred in VEC-richer compounds (VEC $\geq$ 63). For the Ru-rich (VEC-poorer) compounds, Fe has been the magnetically active element and mostly 3d or 4d transition metals have been used on the A site [in $A_2M(TT')_5B_2$]. Consequently, Mn and the 5d element (Hf) should be mostly credited for this unexpected behavior in this VEC-poorer range.

■ ASSOCIATED CONTENT

Supporting Information

The Supporting Information is available free of charge on the ACS Publications website at DOI: 10.1021/acs.inorgchem.7b01758.

Listings of crystal and electronic structure data, a Rietveld refinement plot, EDX mapping and spectrum, COHP curves, and molar magnetic susceptibility versus temperature plots (PDF)

■ AUTHOR INFORMATION

Corresponding Author

*E-mail: bfokwa@ucr.edu.

ORCID

Mikhail E. Itkis: 0000-0003-2447-2267

Boniface P. T. Fokwa: 0000-0001-9802-7815

Notes

The authors declare no competing financial interest.

■ ACKNOWLEDGMENTS

This work was supported by a startup fund to B.P.T.F. at the University of California (UC) at Riverside and the National Science Foundation Career Award to B.P.T.F. (Award DMR-1654780). We acknowledge the San Diego Supercomputer Center and the High-Performance Computing Center at UC Riverside for providing computing resources.

■ REFERENCES

(1) DiSalvo, F. J. Challenges and opportunities in solid-state chemistry. *Pure Appl. Chem.* **2000**, *72*, 1799–1807.

(2) Jansen, M. A concept for synthesis planning in solid-state chemistry. *Angew. Chem., Int. Ed.* **2002**, *41*, 3746–3766.

(3) Kanatzidis, M. G.; et al. Report from the third workshop on future directions of solid-state chemistry: The status of solid-state chemistry and its impact in the physical sciences. *Prog. Solid State Chem.* **2008**, *36*, 1–133.

(4) Yaghi, O. M.; O'keeffe, M.; Ockwig, N. W.; Chae, H. K.; Eddaoudi, M.; Kim, J. Reticular synthesis and the design of new materials. *Nature* **2003**, *423*, 705–714.

(5) Bocarsly, J. D.; Levin, E. E.; Garcia, C. A.; Schwennicke, K.; Wilson, S. D.; Seshadri, R. A Simple Computational Proxy for Screening Magnetocaloric Compounds. *Chem. Mater.* **2017**, *29*, 1613–1622.

(6) Canfield, P. C. Fishing the Fermi sea. *Nat. Phys.* **2008**, *4*, 167–169.

(7) Scheifers, J. P.; Zhang, Y.; Fokwa, B. T. P. Boron: Enabling exciting metal-rich structures and magnetic materials. *Acc. Chem. Res.* **2017**, *50*, 2317.

(8) Park, H.; Misse, P.; Mbarki, M.; Shankhari, P.; Fokwa, B. T. P. Synthesis and magnetic properties of the new boride series $MRh_{6-n}Ru_nB_3$ (M= Co, Ni; n= 1–5). *Eur. J. Inorg. Chem.* **2017**, DOI: 10.1002/ejic.201700418.

(9) Shankhari, P.; Misse, P. R.; Mbarki, M.; Park, H.; Fokwa, B. P. Chemical Tuning of Magnetic Properties through Ru/Rh Substitution in Th_7Fe_3-type $FeRh_{6-n}Ru_nB_3$ (n= 1–5) Series. *Inorg. Chem.* **2017**, *56*, 446–451.

(10) Mbarki, M.; St. Touzani, R.; Fokwa, B. Unexpected Synergy between Magnetic Iron Chains and Stacked B_6 Rings in $Nb_6Fe_{1-x}Ir_{6+x}B_8$. *Angew. Chem., Int. Ed.* **2014**, *53*, 13174–13177.

(11) Hofmann, K.; Kalyon, N.; Kapfenberger, C.; Lamontagne, L.; Zarrini, S.; Berger, R.; Seshadri, R.; Albert, B. Metastable Ni_7B_3: A New Paramagnetic Boride from Solution Chemistry, Its Crystal Structure and Magnetic Properties. *Inorg. Chem.* **2015**, *54*, 10873–10877.

(12) Zheng, Q.; Gumeniuk, R.; Borrmann, H.; Schnelle, W.; Tsirlin, A. A.; Rosner, H.; Burkhardt, U.; Reissner, M.; Grin, Y.; Leithe-Jasper, A.

DOI: 10.1021/acs.inorgchem.7b01758
Inorg. Chem. XXXX, XXX, XXX–XXX

Ternary borides $Nb_7Fe_3B_8$ and $Ta_7Fe_3B_8$ with Kagome-type iron framework. *Dalton Trans.* **2016**, *45*, 9590−9600.
(13) Kuz'ma, Y. B.; Yarmolyuk, Y. P. Crystal structure of the compound $Ti_3Co_5B_2$. *J. Struct. Chem.* **1971**, *12*, 422−424.
(14) Fokwa, B. Transition-Metal-Rich Borides−Fascinating Crystal Structures and Magnetic Properties. *Eur. J. Inorg. Chem.* **2010**, *2010*, 3075−3092.
(15) Nagelschmitz, E.; Jung, W. Scandium Iridium Boride $Sc_3Ir_5B_2$ and the Quaternary Derivatives $Sc_2MIr_5B_2$ with M= Be, Al, Si, Ti, V, Cr, Mn, Fe, Co, Ni, Cu, Ga, or Ge: Preparation, Crystal Structure, and Physical Properties. *Chem. Mater.* **1998**, *10*, 3189−3195.
(16) Dronskowski, R.; Korczak, K.; Lueken, H.; Jung, W. Chemically tuning between ferromagnetism and antiferromagnetism by combining theory and synthesis in iron/manganese rhodium borides. *Angew. Chem., Int. Ed.* **2002**, *41*, 2528−2532.
(17) Fokwa, B.; Lueken, H.; Dronskowski, R. Rational Synthetic Tuning between Itinerant Antiferromagnetism and Ferromagnetism in the Complex Boride Series $Sc_2FeRu_{5-n}Rh_nB_2$ ($0 \leq n \leq 5$). *Chem. - Eur. J.* **2007**, *13*, 6040−6046.
(18) Samolyuk, G. D.; Fokwa, B. P.; Dronskowski, R.; Miller, G. J. Electronic structure, chemical bonding, and magnetic properties in the intermetallic series $Sc_2Fe(Ru_{1-x}Rh_x)_5B_2$ from first principles. *Phys. Rev. B* **2007**, *76*, 1−12.
(19) Fokwa, B.; Lueken, H.; Dronskowski, R. Rational Design of Complex Borides−One-Electron-Step Evolution from Soft to Semi-Hard Itinerant Ferromagnets in the New Boride Series $Ti_2FeRu_{5-n}Rh_nB_2$ ($1 \leq n \leq 5$). *Eur. J. Inorg. Chem.* **2011**, *2011*, 3926−3930.
(20) Hermus, M.; Fokwa, B. Synthesis, Crystal Structure, and Ru/Ir Site Preference in the Complex Boride Series $Ti_2FeRu_{5-x}Ir_xB_2$ and $Zr_2Fe_{1-\delta}Ru_{5-x+\delta}Ir_xB_2$ (x= 1−4, δ< 0.15). *Z. Anorg. Allg. Chem.* **2011**, *637*, 947−954.
(21) Hermus, M.; Yang, M.; Grüner, D.; DiSalvo, F. J.; Fokwa, B. P. Drastic Change of Magnetic Interactions and Hysteresis through Site-Preferential Ru/Ir Substitution in $Sc_2FeRu_{5-x}Ir_xB_2$. *Chem. Mater.* **2014**, *26*, 1967−1974.
(22) Ly, V.; Wu, X.; Smillie, L.; Shoji, T.; Kato, A.; Manabe, A.; Suzuki, K. Low-temperature phase MnBi compound: A potential candidate for rare-earth free permanent magnets. *J. Alloys Compd.* **2014**, *615*, S285−S290.
(23) Kim, S.-H.; Boström, M.; Seo, D.-K. Two-Dimensional Superdegeneracy and Structure− Magnetism Correlations in Strong Ferromagnet, Mn_2Ga_5. *J. Am. Chem. Soc.* **2008**, *130*, 1384−1391.
(24) Ma, S.; Bao, K.; Tao, Q.; Zhu, P.; Ma, T.; Liu, B.; Liu, Y.; Cui, T. Manganese mono-boride, an inexpensive room temperature ferromagnetic hard material. *Sci. Rep.* **2017**, *7*, 43759.
(25) Hermus, M.; Fokwa, B. Experimental and First-Principles Studies of the Ternary Borides $Ta_3Ru_5B_2$ and $M_{3-x}Ru_{5+x}B_2$ (M= Zr, Hf). *Eur. J. Inorg. Chem.* **2014**, *2014*, 3085−3094.
(26) Blöchl, P. E. Projector augmented-wave method. *Phys. Rev. B: Condens. Matter Mater. Phys.* **1994**, *50*, 17953−17979.
(27) Kresse, G.; Joubert, D. From ultrasoft pseudopotentials to the projector augmented-wave method. *Phys. Rev. B: Condens. Matter Mater. Phys.* **1999**, *59*, 1758−1775.
(28) Kresse, G.; Furthmüller, J. Efficient iterative schemes for ab initio total-energy calculations using a plane-wave basis set. *Phys. Rev. B: Condens. Matter Mater. Phys.* **1996**, *54*, 11169−11186.
(29) Brgoch, J.; Yeninas, S.; Prozorov, R.; Miller, G. J. Structure, bonding, and magnetic response in two complex borides: $Zr_2Fe_{1-\delta}Ru_{5+\delta}B_2$ and $Zr_2Fe_{1-\delta}(Ru_{1-x}Rh_x)_{5+\delta}B_2$. *J. Solid State Chem.* **2010**, *183*, 2917−2924.
(30) Zhang, Y.; Miller, G. J.; Fokwa, B. P. Computational Design of Rare-Earth-Free Magnets with the $Ti_3Co_5B_2$-Type Structure. *Chem. Mater.* **2017**, *29*, 2535−2541.
(31) Young, D. S.; Sachais, B. S.; Jefferies, L. C. The Rietveld method, 1993.
(32) Rodriguez-Carvajal, J. FULLPROF: a program for Rietveld refinement and pattern matching analysis. *Satellite meeting on powder diffraction of the XV congress of the IUCr*, Toulouse, France, 1990; Vol. *127*.
(33) Dronskowski, R.; Korczak, K.; Lueken, H.; Jung, W. Chemically tuning between ferromagnetism and antiferromagnetism by combining theory and synthesis in iron manganese rhodium borides. *Angew. Chem., Int. Ed.* **2002**, *41*, 2528−2532.

DOI: 10.1021/acs.inorgchem.7b01758
Inorg. Chem. XXXX, XXX, XXX−XXX